

## Theoretical and experimental study of current–voltage characteristics of asymmetric bipolar membranes

Stanislav Sergeevich Melnikov\*, Nicolay Victorovich Sheldeshov, Victor Ivanovich Zabolotskii

Kuban State University, Stavropolskaya 149, 350040 Krasnodar, Russia, Tel. +7 (961) 5929147; email: melnikov.stanislav@gmail.com (S.S. Melnikov), Tel. +8 (861) 2199573; email: sheld\_nv@mail.ru (N.V. Sheldeshov), Tel. +7 (988) 2450407; email: vizab@chem.kubsu.ru (V.I. Zabolotskii)

Received 23 November 2017; Accepted 21 June 2018

---

### ABSTRACT

A mathematical model describing the transfer of hydrogen and hydroxyl ions and ions of salt through asymmetric bipolar membranes is developed. The model accounts for an electrochemical reaction, which is water splitting at the boundary between an anion-exchange and a cation-exchange layers. The chemical reaction causes the occurrence of the overvoltage of the bipolar region, which leads to a deviation of the current–voltage characteristics of the bipolar membrane from linearity. We have demonstrated bifunctionality of the asymmetric bipolar membranes, their ability to transport ions of salt and water dissociation products simultaneously, both experimentally and theoretically. Depending on their structure and the external conditions, the first or the second function may be dominant. In dilute solutions, water dissociation occurs with high current efficiency, and in the concentrated solutions, there is a simultaneous transfer of salt ions, as well as water splitting products.

*Keywords:* Current–voltage characteristic; Asymmetric bipolar membrane; Surface modification; Bilayer membrane; Mathematical modeling

---

### 1. Introduction

Bipolar membranes are bilayer composites consisted of a cation-exchange and an anion-exchange layers connected in series. The unique feature of bipolar membranes is that primary charge carriers in them are hydrogen and hydroxyl ions, which appear at the bipolar boundary as a result of the water-splitting reaction [1]. As a result, the processes of conversion of salts into the corresponding acids and bases with the use of bipolar membranes have been developed [2–4].

Due to the presence of coions in monopolar (cation-exchange and anion-exchange) layers of bipolar membranes there is an asymmetry of salt ions fluxes through bipolar membrane [5]. It is possible to control the amount of salt ions transferred across the bipolar membrane

by changing the thickness of the monopolar layers [6]. Membranes, in which the cation- and anion-exchange layers have different thicknesses, will henceforth be called asymmetric bipolar membranes. The application of a thin charged film [6,7] or an ion-exchange suspension [8] onto the surface of the monopolar membrane allows obtaining an asymmetric bipolar membrane with high permeability for salt ions. This method is commonly used for the preparation of membranes selective toward monovalent ions [9–11]. At the same time, such membrane acquires the water splitting ability due to the formation of a bipolar boundary at the interface between the cation-exchange and anion-exchange layers. The advantage of the asymmetric bipolar membrane is the possibility to regulate the ratio of the transport functions of salt ions and the generation of water-splitting products.

Depending on the properties of the membrane substrate, the thickness of the modifying film, and the nature of the water-splitting catalyst, the properties of the asymmetric bipolar membrane can vary widely [7]. One must also take

---

\* Corresponding author.

into account that the properties of an external solution also affect the electrochemical behavior of the asymmetric bipolar membrane. An instrument is required that will allow us to predict the properties of the asymmetric bipolar membrane with an optimal set of parameters for a specific electromembrane process. One of the ways to solve this problem can be the accumulation of experimental data and its analysis. The second way is to develop a mathematical model that describes the behavior of the membrane in the electrolyte solution. It is convenient to use the current–voltage characteristic of the membrane to compare the membranes with each other and predict their behavior.

The method of voltammetry makes it possible to qualitatively study the process of ions transport through the bipolar membrane (BPM). The shape of the current–voltage characteristic is determined by the structure of the membrane and by the nature of the processes occurring in it under polarization causing by an electric current. The potential drop across the membrane is the sum of several components: the Donnan potentials at the membrane solution boundaries, the ohmic potential drop across the monopolar layers, and the potential drop at the bipolar boundary.

The number of theoretical papers devoted to the transfer of ions through bipolar membranes is quite large [12–24]. Historically, the first hypothesis was that in the bipolar region there is a direct contact between the cation-exchange and anion-exchange layer and a space charge region appears on this boundary, which is analogous to the PN junction in semiconductors [12]. Later, it was shown that the structure of the bipolar region is more complicated [18]. According to modern concept, the bipolar membrane consists of at least three layers [24]: the cation-exchange and anion-exchange layers, and a thin intermediate layer between them. It is in the intermediate layer (bipolar boundary) that the water dissociation reaction proceeds. It is worth noting that in the work of Femmer et al. [24], the model proposed by the authors is taking into account the violation of the condition of electro-neutrality at the interface between the cation-exchange and anion-exchange layers.

It is also worth noting that most of the known models do not take into account ion transport in the diffusion layers located near the bipolar membrane. The effect of diffusion layers on the current–voltage characteristic of a bipolar membrane was taken into account only in Refs. [22,24]. Allowance for diffusion layers is especially important when the diffusion saturation in the cation-exchange and/or anion-exchange layer of the bipolar membrane is comparable with the saturation of diffusion in the diffusion layer in the external solution. There is an experimental evidence that the magnitude of the limiting electrodiffusion current on a bipolar membrane can be controlled by changing the thickness [7] or the charge [6] of the monopolar layers of the bipolar membrane. A theoretical description of the two above factors was given by Xu [21].

A common drawback of these works is that the water-splitting reaction proceeding at the bipolar boundary is considered as a “fast” reaction. On the one hand, this allows to use the quasi-equilibrium condition ( $c_{\text{H}^+} \times c_{\text{OH}^-} = 10^{-14}$ ) at any point inside the electromembrane system, which greatly simplifies the problem. At the same time, this formulation of the problem does not take into account the chemical

overvoltage arising in the bipolar membrane as a result of the slow chemical reaction which is the water-splitting reaction.

The effect of the electric field on the rate of the water dissociation reaction within the framework of the second Wine effect was taken into account in Refs. [16,17,23]. At the same time in Ref. [25] Simons showed that the water-splitting reaction in the electromembrane system can proceed through a catalytic mechanism involving ionogenic groups of the membrane. Subsequently, the theory of the catalytic character of the water dissociation reaction was developed by Zabolotskii [26], Umnov [19], Timashev [27], and Tanaka [28].

The purpose of this work is a theoretical and experimental study of the current–voltage characteristics of asymmetric bipolar membranes under various conditions.

## 2. Experimental

### 2.1. Materials

#### 2.1.1. Asymmetric bipolar membranes

Asymmetric bipolar membranes with different thicknesses of the cation-exchange layer were obtained by the method described in Ref. [7]. The thickness of the cation-exchange film was controlled by a micrometer Coolant Proof Micrometer Series 293. Some physicochemical properties of the studied membranes are provided in Table 1.

The cation-exchange layer was formed from precursor LF-4SC. The LF-4SC was commercially obtained from LLC Plastpolimer-Prom, Russia. Anion-exchange membrane (Ralex AMH-Pes) was commercially obtained from Mega a.s., Czech Republic.

Asymmetric bipolar membranes with 10, 30, 50, and 70  $\mu\text{m}$  thick cation-exchange layer were used to study the influence of the thickness on the electrochemical and transport characteristics of a bipolar membrane.

#### 2.1.2. Bipolar membranes

To verify the adequacy of the model, previously obtained data for heterogeneous bipolar membranes MB-1, MB-2, and MB-3 were used. The current–voltage characteristics of these membranes were obtained in Ref. [19], their features are given in Ref. [1].

Table 2 lists some of the physicochemical properties of these membranes.

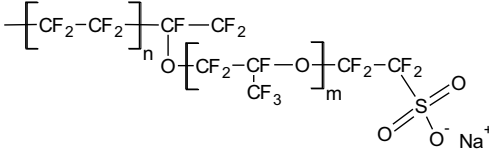
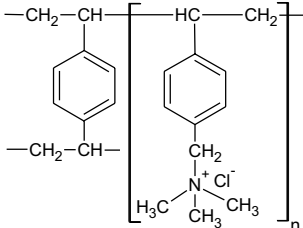
#### 2.1.3. Chemicals

The chemicals used in the experiments include: hydrochloric acid, sodium hydroxide, and sodium nitrate. All reagents were supplied by LLC Medlex (Russia). All reagents were of an analytical grade. Deionized water was used for preparation of the solutions throughout all experiments.

### 2.2. Voltammetry

The current–voltage characteristic of a bipolar membrane has some specific features in comparison with the current–voltage characteristic of a monopolar membrane. In particular, the current–voltage characteristics of a bipolar

Table 1  
Physicochemical properties of monopolar layers forming an asymmetric bipolar membrane

Property	Cation-exchange layer	Anion-exchange layer
Membrane	MF-4SC	Ralex AMH-Pes
Polymeric matrix	Polytetrafluoroethylene	Polystyrene divinylbenzene
Elementary cell		
Inert binder	–	Polyethylene
Reinforcing mesh	–	Polyester
Wet thickness, mm	0.01–0.07 <sup>a</sup>	0.65
Counterion transport number (1.0/0.5 M NaCl)	> 0.94	> 0.95 [29]
Ion-exchange capacity, mmol/g-dry	0.9	1.6 [29]
Water uptake, %	22	32

<sup>a</sup>The thickness of the cation-exchange layer was set individually for each membrane.

Table 2  
Physicochemical properties of monopolar layers forming an asymmetric bipolar membrane

Property	MB-1	MB-2	MB-3
Polymeric matrix	Polystyrene divinylbenzene		
Inert binder	Polyethylene		
Reinforcing mesh	Polyamide		
Wet thickness <sup>a</sup> , mm	0.9 ± 0.3		
Ion-exchange capacity, mmol/g-dry:			
Cation-exchange layer	1.4	1.4	1.9
Anion-exchange layer	4.3	1.4	1.4
Ionic group:			
Cation-exchange layer	–SO <sub>3</sub> H	–SO <sub>3</sub> H	–PO <sub>3</sub> H <sub>2</sub>
Anion-exchange layer	≡N, =NH	–N(CH <sub>3</sub> ) <sub>3</sub>	–N(CH <sub>3</sub> ) <sub>3</sub>
Potential drop, V ( <i>i</i> = 4 A/dm <sup>2</sup> in 0.5 M NaCl)	5.8	13.5	3.8

<sup>a</sup>Varies between batches.

membrane measured in salt solution and an acid-alkali system (where bipolar membrane is placed between acidic solution from the cation-exchange layer side and alkali from the anion-exchange layer side) differ in shape (Fig. 1). In the acid-alkali system, the ohmic region and the plateau of the limiting current are, as a rule, absent and can be found only in concentrated solutions (1 M and higher).

It can be seen from Fig. 1(a) that when the membrane is in the so-called “reverse current bias” the counterions on each of both sides of the membrane move to the corresponding electrodes. In this case, the monopolar layers of the membrane prevent the transfer of coions (salt ions) through the membrane. As a result, even at very low values of the polarizing current, the limiting state is reached. The further buildup of the current leads to the removal of mobile ions from the

bipolar boundary region, the formation of a space charge region, and the initiation of a water dissociation reaction. The appearance of new charge carriers leads to a deviation of the shape of the current–voltage characteristic from the linear plateau. In the case of concentrated solutions of acid and alkali, the contribution of coions electrodiffusion through the monopolar layers becomes much more significant, owing to which it is possible to fix the ohmic region and the plateau of the limiting current of the current–voltage characteristic in some bipolar membranes.

In the case of measuring the current–voltage characteristic in an electromembrane system in which an asymmetric bipolar membrane is placed in a saline solution, it is also possible to study the electrodiffusion of salt ions through a bipolar membrane, because, in this case, the monopolar

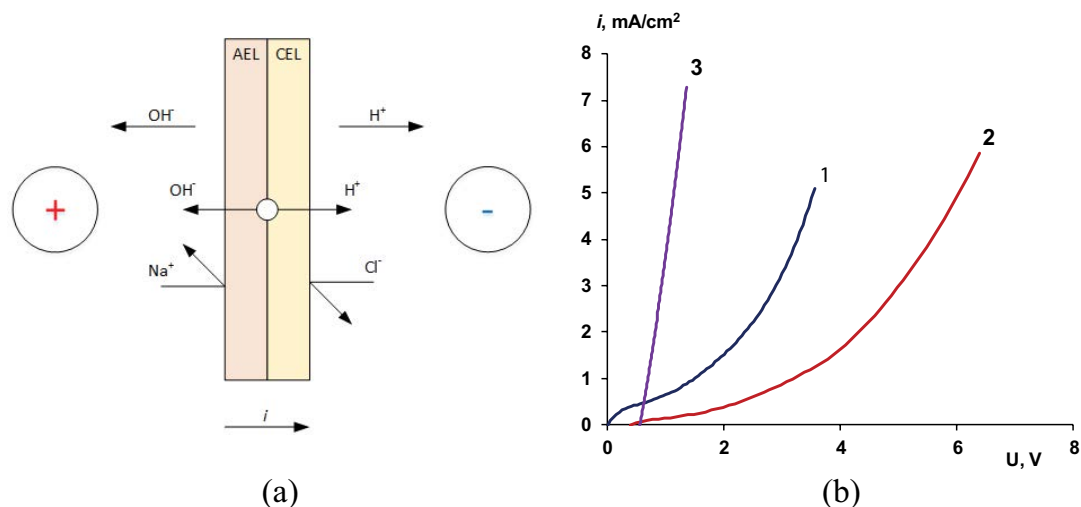


Fig. 1. Scheme of the ion transport in the electromembrane system with bipolar membrane in the reverse current bias mode (a); General current-voltage characteristic (b) of the asymmetric bipolar membrane with 30  $\mu\text{m}$  thick CEL measured in a 0.01 M NaCl solution (1) and in a 0.01 M NaOH | asymmetric bipolar membrane | 0.01 M hydrochloric acid system (2), and for an asymmetric bipolar membrane with water-splitting catalyst measured in the same acid-alkali system (3).

layers of the membrane are not in the  $\text{H}^+/\text{OH}^-$  form, but in the form of salt ions. In this case, a small transfer of coions through the membrane when it is polarized by current compensates for their loss from the ion-exchanger material. It should be noted that the value of the limiting current measured in the acid-alkali system will be lower than in the salt solution (Fig. 1(b) curves 1, 2).

Another peculiarity is that the current-voltage characteristic of a bipolar membrane in the acid-alkali system at small values of the polarizing current shows a significant deviation of the potential from zero (Fig. 1(b) curves 2, 3). This is primarily due to the high value of the Donnan potential at the bipolar boundary. For a highly selective bipolar membrane, this potential should be close to the value of the equilibrium potential (0.83 V for the membrane found in the 1 M solution of acid and alkali). One can judge the catalytic activity of the membrane in the water dissociation reaction by the value of the potential of the beginning of water dissociation. The closer this potential to the equilibrium is, the higher the activity is, and vice versa.

A dynamic method was used to measure the current-voltage characteristic of an asymmetric bipolar membrane. Current-voltage characteristics were measured in a four-chamber cell (Fig. 2). The cell was fed with solutions of hydrochloric acid, sodium hydroxide, and sodium nitrate (for electrode chambers washing). A solution of sodium nitrate was used to wash the electrode chambers to prevent the flow of electrode reactions involving solution ions.

Before the measurement the studied membrane was equilibrated with working solutions of acid and alkali, after which a linearly increasing and decreasing current were applied to the cell, and the current-voltage characteristic was recorded. The rate of change of current was  $2 \times 10^{-5}$  A/s. Measurement of the potential difference on the membrane under investigation was carried out with the help of Haber-Lugginn capillaries connected to an Ag/AgCl reference electrodes (in 3 M KCl).

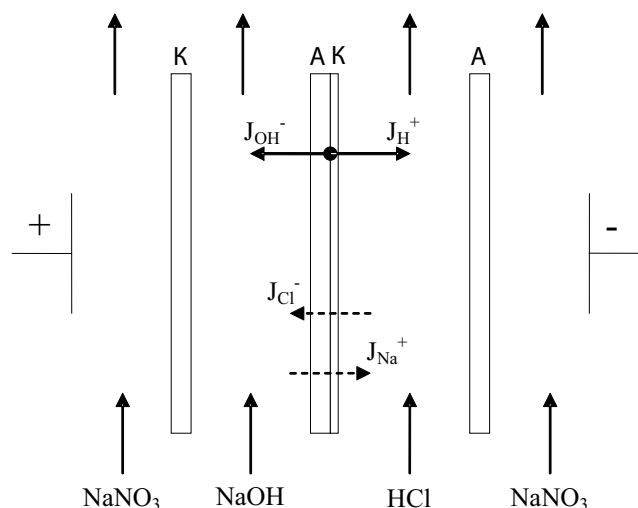


Fig. 2. Scheme of the experimental cell. K – cation-exchange membrane MK-40; A – anion-exchange membrane MA-41; AK – asymmetric bipolar membrane under investigation.

### 3. Theory

#### 3.1. Model formulation

The system under investigation consists of an asymmetric bipolar membrane with different thicknesses ( $d_a, d_c$ ) of the anion-exchange (layer 2) and the cation-exchange (layer 3) layers. The anion-exchange layer is in contact with an alkali solution (sodium hydroxide) and the cation-exchange layer is in contact with an acid solution (hydrochloric acid). Both solutions contain a small amount of salt ions (sodium in acid and chloride in alkali). Concentrations of solutions on both sides of the membrane are assumed to be the same. There are diffusion boundary layers of equal thickness  $\delta$  (layers 1

and 4) on both sides of the membrane in the solutions. The current flows through the system in such a way that the membrane is in the reverse current bias mode (Fig. 3).

The problem is stated as a direct boundary value problem, that is, it is required to obtain the current–voltage characteristic of the membrane on the given parameters of the initial model.

In each of the four layers, the transfer of each of the ions ( $i = C, A, H, OH$ ) is described by the Nernst–Planck equations:

$$j_i = -D_i \left( \frac{dc_i}{dx} + \frac{z_i F}{RT} c_i \frac{d\varphi}{dx} \right) \quad (1)$$

The stationarity condition of the transfer is satisfied for each of the ions (the equality of the ion fluxes in the membrane and in the solution):

$$\frac{d\bar{j}_i}{dx} = \frac{dj_i}{dx} = v_i \quad (2)$$

For salt ions  $v_C = v_A = 0$ , and for hydrogen and hydroxyl  $v_H = v_{OH} = v$ , where  $v$  is the rate of water dissociation per unit volume.

Also the electroneutrality condition is satisfied:

$$\sum z_i c_i \pm c_f^j = 0 \quad (3)$$

where  $c_f^j$  – concentration of the fixed ions in the CEL ( $c_f^c$ ) and the AEL ( $c_f^a$ ), for diffusion layers  $c_f^j = 0$ .

The condition of local chemical equilibrium of water ions is also satisfied in all the layers and on the interfaces:

$$c_H c_{OH} = K_w \quad (4)$$

The system of Eqs. (1)–(4) is supplemented by the boundary conditions (5)–(8):

on the left-hand side ( $x_b$ ):

$$c_i(-d_a - \delta) = c_i^b \quad (5)$$

$$\varphi(-d_a - \delta) = 0 \quad (6)$$

on the right-hand side ( $x_a$ ):

$$c_i(d_c + \delta) = c_i^a \quad (7)$$

$$\varphi(d_c + \delta) = U \quad (8)$$

Equilibrium at all interphase boundaries is established according to the Donnan equation:

$$c_i(x_n - 0) e^{\varphi(x_n - 0)} = c_i(x_n + 0) e^{\varphi(x_n + 0)} \quad (9)$$

where  $n = l, r, 0$  (left and left membrane | solution interfaces, bipolar boundary).

The current passing through the system may be expressed in terms of the ionic fluxes:

$$i = F \sum_i z_i j_i \quad (10)$$

Total current passing through the system is due to the transfer of water-splitting products and salt ions:

$$i = i_H + i_{OH} + i_C + i_A \quad (11)$$

For simplicity we will introduce  $i_W = i_H + i_{OH}$  and  $i_S = i_C + i_A$  then:

$$i = i_W + i_S \quad (11a)$$

By combining Eq. (1) with Eq. (10) we obtain:

$$i_W = F(j_{H^+} - j_{OH^-}) = -F \left[ D_H \frac{dc_H}{dx} - D_{OH} \frac{dc_{OH}}{dx} + (D_H c_H + D_{OH} c_{OH}) \frac{d\psi}{dx} \right] \quad (12a)$$

$$i_C = -F \left[ D_C \frac{dc_C}{dx} + D_C c_C \frac{d\psi}{dx} \right] \quad (12b)$$

$$i_A = -F \left[ D_A \frac{dc_A}{dx} - D_A c_A \frac{d\psi}{dx} \right] \quad (12c)$$

where  $\psi = \frac{F}{RT} \varphi$  is the reduced potential.

From Eq. (12) taking into account Eq. (3) we can find:

$$\frac{1}{c_H} \frac{dc_H}{dx} = -\frac{1}{c_{OH}} \frac{dc_{OH}}{dx} = -\frac{i_W}{F(D_H c_H + D_{OH} c_{OH})} - \frac{d\psi}{dx} \quad (13a)$$

$$\begin{aligned} \frac{dc_C}{dx} &= -\frac{i_C}{F D_C} - c_C \frac{d\psi}{dx}, \\ \frac{dc_A}{dx} &= \frac{i_A}{F D_A} + c_A \frac{d\psi}{dx} \end{aligned} \quad (13b)$$

### 3.2. The catalytic nature of the water-splitting reaction

For the first time the catalytic character of the water-splitting reaction at the membrane/solution boundary was proposed by Simons in Ref. [25]. The essence of this approach is that the water-splitting reaction at the interphase boundary proceeds according to two stage protonation–deprotonation mechanism involving ionogenic groups of the membrane. Subsequently, the approach proposed by Simons was used

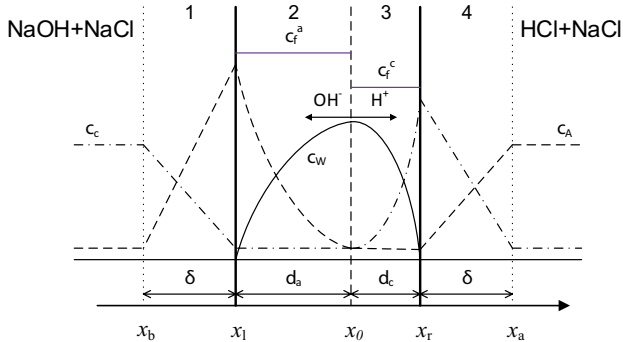


Fig. 3. Bipolar membrane with adjacent diffusion boundary layers. 1, 4 – diffusion boundary layers, 2 – anion-exchange layer, 3 – cation-exchange layer,  $c_f^c, c_f^a$  – concentration of fixed groups in the monopolar layers,  $c_c, c_a, c_w$  – concentrations of cations, anions and products of water splitting, respectively.

in the work of Zabolotskii, Sheldeshov, and Gnusin [26]. In general, this mechanism is represented by reactions:



where AH – acidic fixed group, B – base fixed group.

Note that the forward reaction of the second stage is a rate limiting step, which determines the overall kinetics of the process and the  $k_2$  and the  $k_4$  are the rate limiting constants. Note also, that an autoprotolysis of water must be taken into account:



Considering Eqs. (14)–(16) one can write the fluxes for  $\text{H}^+$  and  $\text{OH}^-$  ions in the CEL:

$$\frac{dj_{\text{H}^+}}{dx} = \frac{dj_{\text{OH}^-}}{dx} = \frac{k_1 k_2 c_f^c c_{\text{H}_2\text{O}}^2 - k_{-1} k_{-2} c_f^c c_{\text{H}^+} c_{\text{OH}^-}}{(k_1 + k_2) c_{\text{H}_2\text{O}} + k_{-1} c_{\text{H}^+} + k_{-2} c_{\text{OH}^-}} + k_d c_{\text{H}_2\text{O}} - k_r c_{\text{H}^+} c_{\text{OH}^-} \quad (17a)$$

and in the AEL:

$$\frac{dj_{\text{H}^+}}{dx} = \frac{dj_{\text{OH}^-}}{dx} = \frac{k_3 k_4 c_f^a c_{\text{H}_2\text{O}}^2 - k_{-3} k_{-4} c_f^a c_{\text{H}^+} c_{\text{OH}^-}}{(k_3 + k_4) c_{\text{H}_2\text{O}} + k_{-3} c_{\text{OH}^-} + k_{-4} c_{\text{H}^+}} + k_d c_{\text{H}_2\text{O}} - k_r c_{\text{H}^+} c_{\text{OH}^-} \quad (17b)$$

Now we can introduce effective constants of water dissociation and recombination in the CEL:

$$k_d^{\text{CEL}} = \frac{k_1 k_2 c_{\text{H}_2\text{O}}}{(k_1 + k_2) c_{\text{H}_2\text{O}} + k_{-1} c_{\text{H}^+} + k_{-2} c_{\text{OH}^-}} + \frac{k_d}{c_f^c} \quad (18a)$$

$$k_r^{\text{CEL}} = \frac{k_{-3} k_{-4} c_f^c}{(k_1 + k_2) c_{\text{H}_2\text{O}} + k_{-1} c_{\text{H}^+} + k_{-2} c_{\text{OH}^-}} + k_r \quad (18b)$$

and in the AEL:

$$k_d^{\text{AEL}} = \frac{k_3 k_4 c_{\text{H}_2\text{O}}}{(k_3 + k_4) c_{\text{H}_2\text{O}} + k_{-3} c_{\text{OH}^-} + k_{-4} c_{\text{H}^+}} + \frac{k_d}{c_f^a} \quad (19a)$$

$$k_r^{\text{AEL}} = \frac{k_{-3} k_{-4} c_f^a}{(k_3 + k_4) c_{\text{H}_2\text{O}} + k_{-3} c_{\text{OH}^-} + k_{-4} c_{\text{H}^+}} + k_r \quad (19b)$$

Then Eq. (17) is reduced to the following form for the CEL:

$$\frac{dj_{\text{H}^+}}{dx} = \frac{dj_{\text{OH}^-}}{dx} = k_d^{\text{CEL}} c_f^c c_{\text{H}_2\text{O}} - k_r^{\text{CEL}} c_{\text{H}^+} c_{\text{OH}^-} \quad (20a)$$

and for the AEL:

$$\frac{dj_{\text{H}^+}}{dx} = \frac{dj_{\text{OH}^-}}{dx} = k_d^{\text{AEL}} c_f^a c_{\text{H}_2\text{O}} - k_r^{\text{AEL}} c_{\text{H}^+} c_{\text{OH}^-} \quad (20b)$$

We introduce a number of assumptions that make it possible to simplify the expressions obtained. First, from Ref. [19] it follows, that  $k_1 \gg k_2 \gg k_d$  and  $k_3 \gg k_4 \gg k_d$ . Also inside the SCR  $c_f^c \gg c_{\text{H}^+}$ ,  $c_f^a \gg c_{\text{H}^+}$  and  $c_f^c \gg c_{\text{OH}^-}$ ,  $c_f^a \gg c_{\text{OH}^-}$ . Then  $k_1 c_{\text{H}_2\text{O}} > (k_{-1} c_{\text{H}^+} + k_{-2} c_{\text{OH}^-})$  and  $k_3 c_{\text{H}_2\text{O}} > (k_{-3} c_{\text{OH}^-} + k_{-4} c_{\text{H}^+})$ . Taking into account the aforesaid, we obtain for the CEL:

$$k_d^{\text{CEL}} \cong k_2 \quad (21a)$$

$$k_r^{\text{CEL}} \cong \frac{k_{-3} k_{-4} c_f^c}{k_1 c_{\text{H}_2\text{O}}} + k_r \quad (21b)$$

and for the AEL:

$$k_d^{\text{AEL}} \cong k_4 \quad (21c)$$

$$k_r^{\text{AEL}} \cong \frac{k_{-3} k_{-4} c_f^a}{k_3 c_{\text{H}_2\text{O}}} + k_r \quad (21d)$$

In the bipolar membrane, the water-splitting reaction takes place at the bipolar junction, hence ionic groups of both the CEL and the AEL participate in the reaction. At some point  $x$  inside the SCR the current is carried by hydrogen and hydroxyl ions so we may write:

$$i_w(x) = F(j_{\text{H}^+}(x) - j_{\text{OH}^-}(x)) = F\left(\int_{-\lambda^{\text{AEL}}}^{\lambda^{\text{CEL}}} \frac{dj_{\text{H}^+}}{dx} dx + \int_{-\lambda^{\text{AEL}}}^{\lambda^{\text{CEL}}} \frac{dj_{\text{OH}^-}}{dx} dx\right) \quad (22)$$

where  $\lambda^{\text{AEL}}$  and  $\lambda^{\text{CEL}}$  are the thicknesses of the SCR in the anion-exchange layer and in the cation-exchange layer.

Outside the SCR the water-splitting reaction does not occur and fluxes are constant, hence:

$$\left. \frac{dj_{\text{H}^+}}{dx} \right|_{-\lambda^{\text{AEL}}} = 0, \quad \left. \frac{dj_{\text{OH}^-}}{dx} \right|_{\lambda^{\text{CEL}}} = 0 \quad (23)$$

Taking into account Eqs. (20), (21), and (23) from Eq. (22) we get:

$$i_w(x) = F\left(\int_{-\lambda^{\text{AEL}}}^0 k_4 c_f^a c_{\text{H}_2\text{O}} dx + \int_0^{\lambda^{\text{CEL}}} k_2 c_f^c c_{\text{H}_2\text{O}} dx\right) - F\left(\int_{-\lambda^{\text{AEL}}}^0 k_r^{\text{AEL}} c_{\text{H}^+} c_{\text{OH}^-} dx + \int_0^{\lambda^{\text{CEL}}} k_r^{\text{CEL}} c_{\text{H}^+} c_{\text{OH}^-} dx\right) \quad (24)$$

The second term in Eq. (24) describes the recombination current of hydrogen and hydroxyl ions back into the water molecules, in what follows we denote:

$$i_r(x) = F\left(\int_{-\lambda^{\text{AEL}}}^0 k_r^{\text{AEL}} c_{\text{H}^+} c_{\text{OH}^-} dx + \int_0^{\lambda^{\text{CEL}}} k_r^{\text{CEL}} c_{\text{H}^+} c_{\text{OH}^-} dx\right) \quad (25)$$

Following [30] we also assume that the rate limiting constants  $k_2$  and  $k_4$  depend exponentially on the electric field strength in the SCR.

$$\begin{aligned} k_2 &= k_{20} \exp[\beta E], \\ k_4 &= k_{40} \exp[\beta E] \end{aligned} \quad (26)$$

where  $k_{20}$  and  $k_{40}$  are the rate limiting constants of reactions (14) and (15) in the absence of an electric ( $i = 0$ );  $\beta$  is the entropy factor.

The electric field strength in the space charge region ( $E(x)$ ) can be found using the Schottky approximation [18]:

$$E(x) = \begin{cases} Fc_f^a(\lambda^{AEL} + x) / \varepsilon\varepsilon_0 & -\lambda^{AEL} \leq x \leq 0 \\ Fc_f^c(\lambda^{CEL} - x) / \varepsilon\varepsilon_0 & 0 \leq x \leq \lambda^{CEL} \end{cases} \quad (27)$$

By changing the variable  $x$  by  $E$  in Eq. (24) using condition (27) we finally obtain:

$$i_w = \varepsilon\varepsilon_0 c_{H_2O} (k_{20} + k_{40}) \left( \int_0^{E_m(\eta_b)} e^{\beta E} dE \right) - i_r \quad (28)$$

where we denote  $k_\Sigma = c_{H_2O} (k_{20} + k_{40})$ .  $k_\Sigma$  is the total effective rate constant of the pseudomonomolecular water dissociation reaction in the space charge region in the absence of an electric field;  $E_m$  is the electric field strength at the interface between phases;  $\eta_b$  is the overvoltage of the bipolar region;  $e$  is the relative permittivity in the space charge region; and  $\varepsilon_0$  is the absolute dielectric constant of vacuum.

Since each of the rate limiting constants ( $k_{20}$ ,  $k_{40}$ ) depends on the chemical nature of the ionogenic groups involved in the reactions similar to (14) and (15), the total constant ( $k_\Sigma$ ) also depends on the chemical nature of the ionogenic groups. The protonation/deprotonation reactions involving ionic groups of the ion exchange membranes studied are described in Appendix A.

### 3.3. The total potential drop in the system

The flow of chemical reactions (14) and (15) at the bipolar boundary leads to the appearance of chemical overvoltage in the membrane system. An expression, which relates the water-splitting products current with an overvoltage arising at the bipolar boundary, can be obtained from Eq. (28). Let us assume that the recombination current in the investigated range of current densities does not change and is equal to its value in the absence of an external electric field:

$$i_r = k_\Sigma \varepsilon\varepsilon_0 \left( \int_0^{E_m(0)} e^{\beta E} dE \right) \quad (29)$$

Substituting Eq. (29) into (28) and integrating the result from  $E_m(\eta_b)$  to  $E_m(0)$  we obtain an equation that relates the current carried by water-splitting products with overvoltage of the bipolar region:

$$i_w = \frac{k_\Sigma \varepsilon\varepsilon_0}{\beta} (e^{\beta E_m(\eta_b)} - e^{\beta E_m(0)}) \quad (30)$$

The electric field strength at the interface between phases can be found [19]:

$$E_m(\eta_b) = \sqrt{\frac{2Fc_f^c c_f^a (\Delta\phi_0 + \eta_b)}{\varepsilon\varepsilon_0 (c_f^c + c_f^a)}} \quad (31a)$$

$$E_m(0) = \sqrt{\frac{2Fc_f^c c_f^a \Delta\phi_0}{\varepsilon\varepsilon_0 (c_f^c + c_f^a)}} \quad (31b)$$

where  $\Delta\phi_0$  is the equilibrium potential of the bipolar boundary:

$$\Delta\phi_0 = \frac{RT}{F} \ln \left( \frac{c_f^c c_f^a}{K_w} \right) \quad (31c)$$

Now the total potential drop across the membrane and two diffusion layers can be expressed as:

$$U = U_m + 2U_\delta \quad (32)$$

where  $U_m$  is the potential drop across bipolar membrane;  $U_\delta$  is the potential drop across diffusion layers.

Potential drop across membrane is a sum of three terms: the ohmic potential drop across CEL and AEL, the Donnan potential on the left-hand side and right-hand side which interface membrane solution, and the bipolar region overvoltage.

$$U_m = U_{Ohm} + \frac{RT}{F} \ln \left( \frac{c_H|_{x=x_r}}{c_H|_{x=x_l}} \right) + \eta_b \quad (33)$$

It is necessary for theoretical calculation of current-voltage characteristics to know a number of parameters of the electromembrane system such as concentration of salt in alkali and acid ( $c_A = c_C = c_S$ ), concentrations of alkali and acid outside the membrane ( $c_w$ ), the thickness of the monopolar layers ( $d_c, d_a$ ), the ion-exchange capacity of each layer ( $c_f^c, c_f^a$ ), the diffusion coefficients of each of the ions in the solution ( $D_i$ ) and in the membrane ( $\bar{D}_i$ ) (for simplicity we considered that  $\bar{D}_i$  is one order of magnitude lower than  $D_i$ ), the thickness of the diffusion layers ( $d$ ). The values of the parameters  $\beta$  and  $k_\Sigma$  in Eq. (30) can be found from the experiment on the spectra of the electrochemical impedance of bipolar membranes [7,19].

Mathematically, the system of Eqs. (12a)–(12c) with boundary conditions (5)–(8) and the additional conditions (11), (30), and (32) is a boundary value problem in the four-layer domain. The solution of the problem consists in integrating the transport equations in separate layers with subsequent cross-linking of the solutions obtained at the phase boundaries. As a result, ionic fluxes, concentration profiles in each of the layers and total potential drop across the electrochemical system can be found. A simple unmodified method of shooting [31] was used for the solution.

## 4. Results and discussion

### 4.1. Model verification

Verification of the model was carried out according to the literature data [32] (Fig. 4) and from the experimental results obtained in this study of asymmetric bipolar membranes (Fig. 5).

The results presented in Fig. 4 show some variation between the theoretical and experimental results. The reason

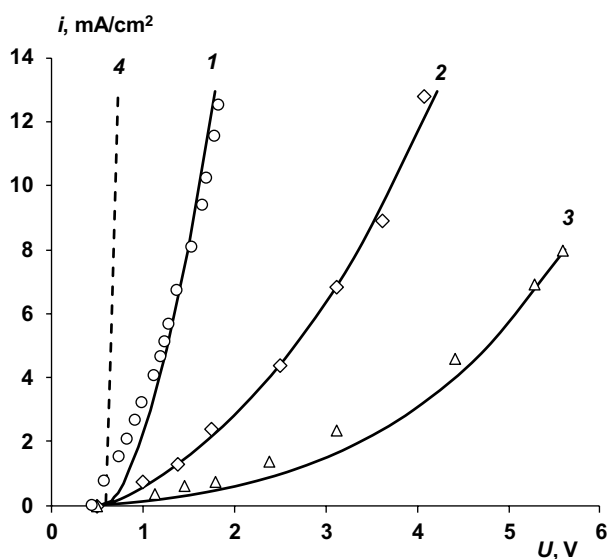


Fig. 4. General current–voltage characteristics of bipolar membranes measured for electromembrane system sodium hydroxide | BPM | hydrochloric acid, obtained in Ref. [32]: 1 – MB-3, 2 – MB-1, 3 – MB-2, 4 – calculation without taking overpotential into account ( $k_{\Sigma} = 10^4 \text{ s}^{-1}$ ). Dots – experimental data, lines – calculated curves. Model parameters (for all membranes):  $c_s = 0.0001 \text{ M}$ ;  $c_w = 0.1 \text{ M}$ ;  $d_c = d_a = 0.45 \text{ mm}$ ;  $c_f^c = c_f^a = 1.5 \text{ M}$ ;  $\delta = 0.16 \text{ mm}$ ; values of  $\beta$  and  $k_{\Sigma}$  are taken from Ref. [19].

for this may be an incomplete correspondence of the embedded model parameters to the experimental conditions. For example, despite being studied by various authors, the ion-exchange capacity of membranes is unknown. Also, the literature does not contain data on hydrodynamic conditions during the experiment, which make it impossible to calculate accurately the thickness of the diffusion layer. All these

factors bring individual errors in the definition of the total potential in the system. Despite this, the obtained theoretical results are in good agreement with experiment. The model makes it possible to calculate the current–voltage characteristics of various bipolar membranes in a wide range of concentrations.

Now let us consider the case when the water-splitting reaction is regarded as a fast reaction and does not cause a rise of the overvoltage at the bipolar boundary. In the framework of our model, this condition is satisfied for values of  $k_{\Sigma}$  greater than  $10^3$ . In reality, such a large value of the effective constant is observed only for certain membranes [20]. A large value of  $k_{\Sigma}$  leads to the fact that the water dissociation products current reaches high values for small values of overvoltage. This can be seen from analysis of Eq. (30), if  $\eta_b \rightarrow 0$  then  $i_w \sim f(k_{\Sigma})$ . In Fig. 4, this state corresponds to curve 4. It is seen that the current–voltage curves obtained for other real membranes, which differ significantly from it. This is especially noticeable in the case of the bipolar membrane MB-2, which has a low activity in the water-splitting reaction. This example shows, as clear as possible, the necessity of taking chemical overvoltage into account in modeling the behavior of bipolar membranes.

The current–voltage characteristics of asymmetric bipolar membranes show a significant decrease in the magnitude of the limiting electrodiffusion current (Fig. 5) as compared with the initial anion-exchange membrane substrate [7]. When the thickness of the cation-exchange layer is  $30 \mu\text{m}$ , the transfer of salt ions through the bipolar membrane decreases substantially, and the limiting current density is only about  $0.05 \text{ mA/cm}^2$ , compared with a limiting current of  $1.2 \text{ mA/cm}^2$  for the anion-exchange membrane substrate measured under the same conditions.

This effect is caused by the fact that the cation exchange layer of MF-4SC “locks” the receiving side of the anion-exchange membrane and prevents the transfer of anions through the bipolar membrane.

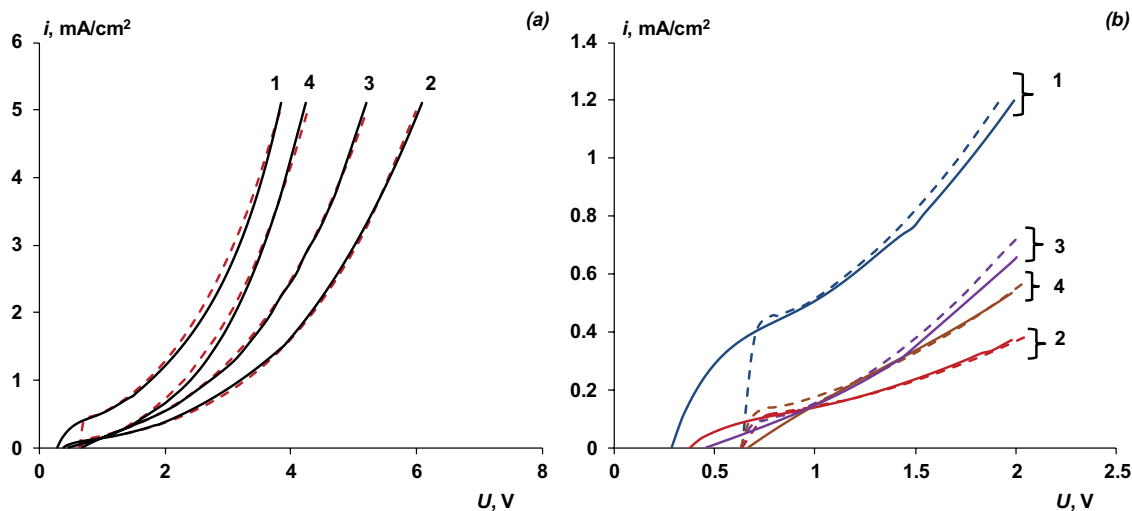


Fig. 5. General current–voltage characteristics of an asymmetric bipolar membranes measured for electromembrane system sodium hydroxide | asymmetric BPM | hydrochloric acid (a) and expanded view of the general current–voltage characteristics up to 2 V (b). CEL thickness ( $d_c$ ), microns: 1 – 10, 2 – 30, 3 – 50, 4 – 70. Lines – experimental data, dashed lines – calculated curves. Model parameters:  $c_s = 0.0001 \text{ M}$ ;  $c_w = 0.01 \text{ M}$ ;  $d_a = 0.45 \text{ mm}$ ;  $c_f^c = 0.9 \text{ M}$ ;  $c_f^a = 1.6 \text{ M}$ ;  $\delta = 0.16 \text{ mm}$ ;  $\beta = 5.6 \times 10^{-9} \text{ m/V}$ ;  $k_{\Sigma} = 3.8 \text{ s}^{-1}$  [33].



The difference in the shape of the current–voltage curves between curve 1 and the remaining membranes can be explained by the fact that with such a small thickness of the modifying layer, the membrane largely preserves the monopolar membrane properties.

It can be seen from the obtained results that the proposed model, with proper selection of the properties of the catalyst (parameters  $\beta$  and  $k_x$ ), describes quite well the current–voltage characteristic of both classical and asymmetric bipolar membranes. It is interesting to study how the parameters of the electromembrane system, primarily the thickness of the cation-exchange layer, the concentration of external solutions and the exchange capacity of the cation exchange layer influence the current–voltage characteristic of the membrane.

When an asymmetric bipolar membrane is placed in a solution with a relatively high concentration (0.5 M), salt transfer rises significantly through the membrane (Fig. 6). The ohmic region that corresponds to the electrodiffusion transfer of salt ions through the cation-exchange and anion-exchange layers of an asymmetric bipolar membrane can be seen (Fig. 6). Just as in the case of a monopolar membrane, the primary charge carriers in the asymmetric bipolar membrane are salt ions within the ohmic region of the current–voltage curve, and the water-splitting reaction does not proceed at the bipolar boundary. The magnitude of the limiting current on the bipolar membrane corresponds to the maximum value of the salt ions flux through the membrane, that is, the higher its value is, the higher the flux of salt ions through the membrane is and, correspondingly, the higher the transfer number of salt ions is. The limiting current increases with decreasing thickness of the modifying cation-exchange layer,

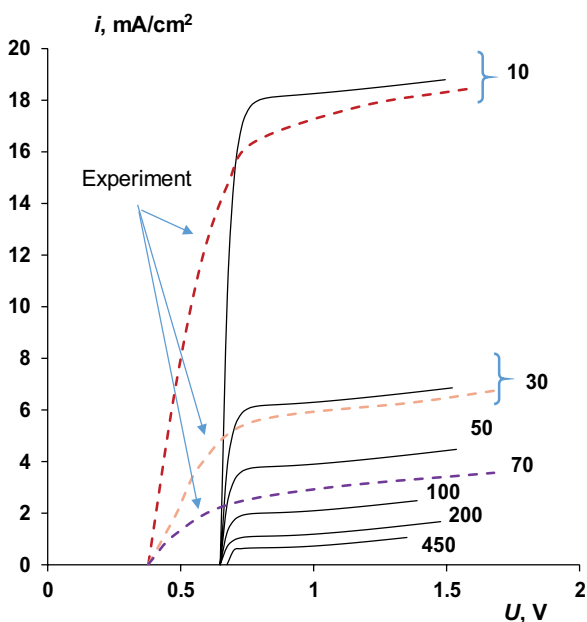


Fig. 6. Initial sections of the current–voltage curves. The numbers next to the curves are the thickness of the cation-exchange layer in microns. Model parameters:  $c_s = 0.0001$  M;  $c_w = 0.5$  M;  $d_a = 0.45$  mm;  $c_f^c = 0.9$  M;  $c_f^a = 1.6$  M;  $\delta = 0.22$  mm;  $\beta = 24 \times 10^{-9}$  mV;  $k_x = 3.8$  s $^{-1}$  [33].

which is apparently associated with an increase in the diffusion permeability of the modifying layer.

Fig. 6 shows that the initial sections of the experimental and calculated volt–ampere curves differ substantially. In particular, a certain slope of the ohmic region is an important characteristic for the experimental curves, as well as a lower value of the equilibrium potential compared with the calculated curve. The first difference can be explained by the fact that on the experimental curve, in addition to the membrane itself and the adjacent diffusion layers, the resistance of the solution that lies in the measuring capillaries and the solution layer between the tip of the capillary and the diffusion layer also contribute. The shift of the equilibrium potential to the region of lower values is explained by the fact that the heterogeneous membranes under investigation have large pores [34] in their structure in which the equilibrium solution is located. Such pores serve as an additional pathway for the nonselective transfer of salt ions, which reduces the concentration of hydrogen and hydroxyl ions at the bipolar boundary and, as a consequence, reduces the equilibrium potential.

The dependence of the limiting electrodiffusion current on the thickness of the modifying film has a nonlinear character (Fig. 7). Moreover, with the increase in the thickness of the cation-exchange layer, it is not possible to exclude the transfer of salt ions completely, as evidenced by the results obtained for the bipolar membrane MB-2, in which the thickness of the cation exchange layer is 450  $\mu$ m.

The same type of dependence can be seen for different CEL ion-exchange capacities (Fig. 8). It can be explained by the fact that a cation-exchange layer with a larger ion-exchange capacity has a larger charge. As a result of the electrostatic interaction between the cation-exchange layer and the anions (coions for a given layer), the force of their repulsion from the surface and the volume of the membrane increase, and it leads to a decrease in the value of the limiting current density.

As shown in Figs. 7 and 8, the magnitude of the limiting current on the asymmetric bipolar membrane depends not only on the thickness of one of the layers but also on its

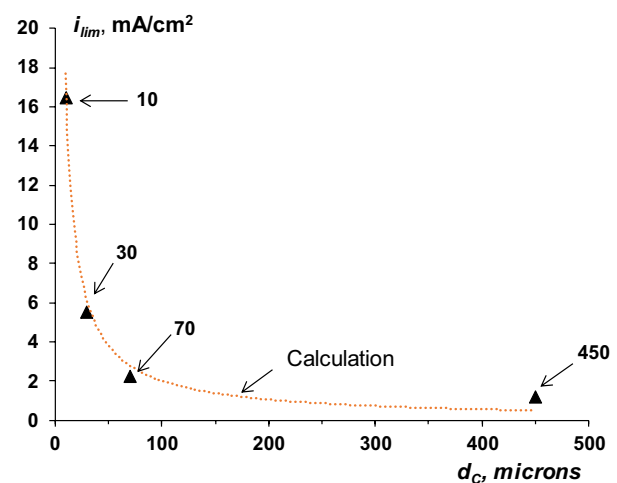


Fig. 7. Dependence of the limiting current value on the CEL thickness. Dots – experimental data; line – calculated curve. Model parameters are the same as in Fig. 6.

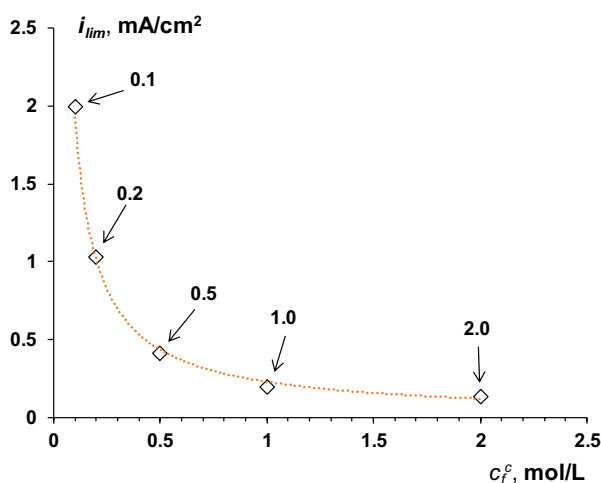


Fig. 8. Dependence of the limiting current value on the CEL ion-exchange capacity. Dots – experimental data; line – calculated curve. Model parameters:  $c_s = 0.0001$  M;  $c_w = 0.01$  M;  $d_a = 0.45$  mm;  $d_c = 0.03$  mm;  $c_f^a = 1.6$  M;  $\delta = 0.16$  mm;  $\beta = 5.16 \times 10^{-9}$  m/V;  $k_{\Sigma} = 3.8$  s<sup>-1</sup> [33].

charge (ion-exchange capacity). The use of commercial liquids from which you can cast a membrane (LF-4SK, Liquion) allows setting only one of these parameters, namely the thickness of a layer. At the same time, the sulfonation procedure of polyether ether ketone is well known and is used by many researchers to produce cation-exchange films and membranes [35–38]. The selection of the sulfonation time, as well as the volume ratio of SPEEK/PEEK, allows setting different values of the ion-exchange capacity of the membrane. From this point of view, the SPEEK is a more suitable modifier than the one used in this work.

The obtained results (Figs. 4–8) show that if the parameters responsible for chemical overvoltage are known, the proposed model can be used to describe the properties of both classical and asymmetric bipolar membranes. It is of interest to use the obtained data to determine these parameters only from the general current–voltage characteristic of the membrane.

#### 4.2. The use of a model for determining the parameters catalytic activity of the functional groups

In Ref. [15], a method for determining the parameters  $\beta$  and  $k_{\Sigma}$  has been proposed; however, a large array of experimental data was required for this. The magnitude of the overvoltage is determined from the spectra of the electrochemical impedance, the fluxes of hydrogen and hydroxyl ions are determined on the basis of the results of measuring the effective ion transport numbers, and it is also necessary to know the current–voltage characteristic of the membrane to construct a partial current–voltage characteristics of the bipolar region. Thus, the definition of these parameters is a time-consuming process.

It was shown above that even the general current–voltage characteristic depends strongly on the values of the indicated parameters. Selecting them to the best coincidence of the calculated current–voltage curve with the experimental one can find the values of the parameters  $\beta$  and  $k_{\Sigma}$ .

Table 3

Values of parameters  $\beta$  and  $k_{\Sigma}$  for bipolar and asymmetric bipolar membranes

Membrane	Partial CVC model [19]		CVC model	
	$k_{\Sigma}$ s <sup>-1</sup>	$\beta \times 10^9$ , m/V	$k_{\Sigma}$ s <sup>-1</sup>	$\beta \times 10^9$ , m/V
MB-1 <sup>a</sup>	8.95	3.65	18	3.4
MB-2 <sup>a</sup>	0.401	7.17	0.9	4.1
MB-3 <sup>a</sup>	248	6.41	150	6
Asymmetric BPM with 30 microns CEL	3.8 <sup>b</sup>	5.16 <sup>b</sup>	1.1	5.6

<sup>a</sup>Data taken from [19]

<sup>b</sup>Data taken from [33]

The results of this selection are given in Table 3. It also contains data on the values of the parameters  $\beta$  and  $k_{\Sigma}$  known from the literature, which were used in the calculations shown in Figs. 4 and 5.

The data in Table 3 show that using the model of the current–voltage characteristic of a bipolar membrane allows one to evaluate the values of the effective rate constants for the dissociation reaction of water and compare them with each other. The obtained results are in qualitative agreement with the literary data [19].

## 5. Conclusion

The electrochemical behavior of asymmetric bipolar membrane depends on its structure (the thickness of the cation-exchange layer) as well as on the conditions of its use (the current density and external solution concentration). In dilute solutions the process of water splitting at the bipolar boundary of the membrane prevails, and an asymmetric bipolar membrane is similar in its properties to a classical bipolar membrane. At low current densities in a more concentrated solution, the asymmetric membrane behaves like a monopolar membrane-substrate, that is, the primary process is the transfer of salt ions.

In comparison with classical bipolar membranes, the lower selectivity (high values of the limiting current) of the asymmetric bipolar membranes is provided due to the small thickness and charge of the cation-exchange layer, which results in a high fraction of the diffusion mechanism of chlorine ion transport in the total mass transfer. One can overcome this issue by changing the chemical nature of the cation-exchange layer. For example, a sulfonated PEEK can be used.

As for the practical aspect, the most interesting mode is the mixed mechanism of ion transport, in which the desalting process can proceed simultaneously with the water-splitting reaction. The role of such processes in the practice of electromembrane technologies is quite high, for example, in the preparation of water for the needs of heat power generation, in the stabilization of juices, wines and other products of the food industry, in the separation of biologically active substances which are sensitive to the pH value.

This work has been supported by Russian Federation president's scholarship program, № SP 1545.2016.1.

## Symbols

$d_a, d_c$	— Thicknesses of the anion-exchange and the cation-exchange layers, m
$\delta$	— The thickness of the diffusion boundary layer, m
$c_f^c, c_f^a$	— Concentrations of fixed groups in the cation-exchange and the anion-exchange layers, mol/m <sup>3</sup>
$c_c, c_a, c_w$	— Concentrations of cations, anions and products of water-splitting, respectively, mol/m <sup>3</sup>
$j_i$	— The flux of species $i$
$c_i$	— The concentration of species $i$ , mol/m <sup>3</sup>
$D_i$	— The diffusion coefficient of species $i$ , m <sup>2</sup> /s
$z_i$	— The valence of species $i$
$F$	— The Faraday constant, A·s/mol
$\phi$	— The electrical potential, V
$v_i$	— The net rate of formation of species by chemical reaction
$K_w$	— Ionic product of water
$i$	— The total current, A/m <sup>2</sup>
$i_H$	— The current carried by hydrogen ions, A/m <sup>2</sup>
$i_{OH}$	— The current carried by hydroxyl ions, A/m <sup>2</sup>
$i_c$	— The current carried by cations, A/m <sup>2</sup>
$i_a$	— The current carried by anions, A/m <sup>2</sup>
$k_\Sigma$	— The total effective rate constant of the pseudomonomolecular water dissociation reaction in the space charge region 2–4 nm thick in the absence of an electric field, s <sup>-1</sup>
$\beta$	— The entropy factor
$E_m$	— The electric field strength at the interface between phases, V/m
$\epsilon$	— The relative permittivity in the space charge region
$\epsilon_0$	— The absolute dielectric constant of vacuum, F/m
$\eta_b$	— The overvoltage of the bipolar region, V
$\Delta\phi_0$	— The equilibrium potential at the bipolar boundary, V
$U_m$	— The potential drop across bipolar membrane, V
$U_\delta$	— The potential drop across diffusion layers, V
CEL	— Cation-exchange layer
AEL	— Anion-exchange layer
BPM	— Bipolar membrane
aBPM	— Asymmetric bipolar membrane

## References

- [1] V. Zabolotskii, N. Sheldeshov, S. Melnikov, Heterogeneous bipolar membranes and their application in electrodialysis, *Desalination*, 342 (2014) 183–203.
- [2] G. Pourcelly, Electrodialysis with bipolar membranes: principles, optimization, and applications, *Russ. J. Electrochem.*, 38 (2002) 919–926.
- [3] T. Xu, Electrodialysis processes with bipolar membranes (EDBM) in environmental protection – a review, *Resour. Conserv. Recycl.*, 37 (2002) 1–22.
- [4] J. Wiśniewski, G. Wiśniewska, T. Winnicki, Application of bipolar electrodialysis to the recovery of acids and bases from water solutions, *Desalination*, 169 (2004) 11–20.
- [5] R. El Moussaoui, G. Pourcelly, M. Maeck, H.D. Hurwitz, C. Gavach, Co-ion leakage through bipolar membranes influence on I-V responses and water-splitting efficiency, *J. Membr. Sci.*, 90 (1994) 283–292.
- [6] J.H. Balster, R. Sumbharaju, S. Srikantharajah, I. Pünt, D.F. Stamatialis, V. Jordan, M. Wessling, Asymmetric bipolar membrane: a tool to improve product purity, *J. Membr. Sci.*, 287 (2007) 246–256.
- [7] V. Zabolotskii, N. Sheldeshov, S. Melnikov, Effect of cation-exchange layer thickness on electrochemical and transport characteristics of bipolar membranes, *J. Appl. Electrochem.*, 47 (2013) 1117–1129.
- [8] O.R. Shendrik, M.I. Ponomarev, V.V. Teselkin, V.D. Grebenyk, Development and properties of cation exchange membranes modified with electrodedated dispersion of anionite, *Khimiya I technology vody*, 7 (1985) 29–32 (in Russian).
- [9] T. Sata, Studies on ion exchange membranes with permselectivity for specific ions in electrodialysis, *J. Membr. Sci.*, 93 (1994) 117–135.
- [10] T.T. Sata, W. Yang, Studies on cation-exchange membranes having permselectivity between cations in electrodialysis, *J. Membr. Sci.*, 206 (2002) 31–60.
- [11] E. Güler, W. van Baak, M. Saakes, K. Nijmeijer, Monovalent-ion-selective membranes for reverse electrodialysis, *J. Membr. Sci.*, 455 (2014) 254–270.
- [12] A. Mauro, Space charge regions in fixed charge membranes and the associated property of capacitance, *Biophys. J.*, 2 (1962) 179–198.
- [13] G. Grossman, Water dissociation effects in ion transport through composite membrane, *J. Phys. Chem.*, 80 (1976) 1616–1625.
- [14] S. Mafe, J.A. Manzanares, P. Ramirez, Model for ion transport in bipolar membranes, *Phys. Rev. A.*, 42 (1990) 6245–6248.
- [15] H. Strathmann, H.-J. Rapp, B. Bauer, C.M. Bell, Theoretical and practical aspects of preparing bipolar membranes, *Desalination*, 90 (1993) 303–323.
- [16] A. Alcaraz, P. Ramirez, S. Mafé, H. Holdik, A simple model for AC impedance spectra in bipolar membranes, *J. Phys. Chem.*, 100 (1996) 15555.
- [17] H. Strathmann, J.J. Krol, H.J. Rapp, G. Eigenberger, Limiting current density and water dissociation in bipolar membranes, *J. Membr. Sci.*, 125 (1997) 123–142.
- [18] V.V. Umnov, N.V. Shel'deshov, V.I. Zabolotskii, Structure of the space-charge region at the anionite-cationite interface in bipolar membranes, *Russ. J. Electrochem.*, 35 (1999) 411.
- [19] V.V. Umnov, N.V. Shel'deshov, V.I. Zabolotskii, Current-voltage curve for the space charge region of a bipolar membrane, *Russ. J. Electrochem.*, 35 (1999) 871.
- [20] H.D. Hurwitz, R. Dibiani, Experimental and theoretical investigations of steady and transient states in systems of ion exchange bipolar membranes, *J. Membr. Sci.*, 228 (2004) 17–43.
- [21] T. Xu, Effect of asymmetry in a bipolar membrane on water dissociation – a mathematical analysis, *Desalination*, 150 (2002) 65–74.
- [22] V.I. Kovalchuk, E.K. Zholkovskij, E.V. Aksenenko, F. Gonzalez-Caballero, S.S. Dukhin, Ionic transport across bipolar membrane and adjacent Nernst layers, *J. Membr. Sci.*, 284 (2006) 255–266.
- [23] T. Xu, R. Fu, A simple model to determine the trends of electric-field-enhanced water dissociation in a bipolar membrane. II. Consideration of water electrotransport and monolayer asymmetry, *Desalination*, 190 (2006) 125–136.
- [24] R. Femmer, A. Mani, M. Wessling, Ion transport through electrolyte/polyelectrolyte multi-layers, *Sci. Rep.*, 5 (2015) 11583.
- [25] R. Simons, Strong electric field effects on proton transfer between membrane-bound amines and water, *Nature*, 280 (1979) 824–826.
- [26] V.I. Zabolotskii, N.V. Shel'deshov, N.P. Gnusin, Dissociation of water molecules in systems with ion-exchange membranes, *Russ. Chem. Rev.*, 57 (1988) 801–808.
- [27] S.F. Timashev, E.V. Kirganova, Mechanism of the electrolytic decomposition of water molecules, bipolar ion-exchange membranes, *Elektrokhimiya*, 17 (1981) 440 (translated *Sov. Electrochem.*, 17 (1981) 366).
- [28] Y. Tanaka, Water dissociation reaction generated in an ion exchange membrane, *J. Membr. Sci.*, 350 (2010) 347–360.
- [29] Heterogenous ion-exchange membranes RALEX. Available at: <http://www.mega.cz/heterogenous-ion-exchangemembranes-ralex.html>.

- [30] S.F. Timashev, Role of temperature and entropic factors in the kinetic of membrane processes, DAN USSR, 285 (1985) 1419–1423 (in Russian).
- [31] V.V. Nikonenko, K.A. Lebedev, S.S. Suleimanov, Influence of the convective term in the Nernst-Planck equation on properties of ion transport through a layer of solution or membrane, Russ. J. Electrochem., 45 (2009) 160–169.
- [32] N.P. Gnusin, V.I. Zabolotckii, N.V. Sheldeshov, V.M. Illarionova, G.Z. Nefedova, I.G. Freidlin, Issledovanie elektrohimicheskikh svoystv promyshlennykh bipoliarnykh membran, Russ. J. Appl. Chem., 53 (1980) 1069–1072 (in Russian).
- [33] S.S. Melnikov, V.I. Zabolotsky, N.V. Sheldeshov, Electrochemical properties of asymmetric bipolar membranes, Condens. Matter Interfaces, 12 (2011) 143–148.
- [34] N. Kononenko, V. Nikonenko, D. Grande, C. Larchet, L. Dammak, M. Fomenko, Y. Volfkovich, Porous structure of ion exchange membranes investigated by various techniques, Adv. Colloid Interface Sci., 246 (2017) 196–216.
- [35] X. Huang, D. Huang, X. Ou, F. Ding, Z. Chen, Synthesis and properties of side-chain-type ion exchange membrane PEEK-g-StSO<sub>3</sub>Na for bipolar membranes, Appl. Surf. Sci., 258 (2012) 2312–2318.
- [36] O.M.M. Kattan Readi, H.J.J. Kuenen, H.J.J. Zwijnenberg, K. Nijmeijer, Novel membrane concept for internal pH control in electro dialysis of amino acids using a segmented bipolar membrane (sBPM), J. Membr. Sci., 443 (2013) 219–226.
- [37] S. Abdu, K. Sricharoen, J.E. Wong, E.S. Muljadi, T. Melin, M. Wessling, Catalytic polyelectrolyte multilayers at the bipolar membrane interface, ACS Appl. Mater. Interfaces, 5 (2013) 10445–10455.
- [38] J. Ran, L. Wu, Y. He, Z. Yang, Y. Wang, C. Jiang, L. Ge, E. Bakangura, T. Xu, Ion exchange membranes: new developments and applications, J. Membr. Sci., 522 (2017) 267–291.

### Appendix A. Protonation–deprotonation reactions involving ionogenic groups of the ion-exchange membrane.

Ionogenic groups	Protonation–deprotonation reactions
–PO <sub>3</sub> H <sub>2</sub>	$-\text{PO}_3\text{H}_2 + \text{H}_2\text{O} \xrightleftharpoons[k_{-1}=10^{10} \pm 10^{11} \text{ L/(mols)}]{k_1=2 \times 10^6 \pm 2 \times 10^7 \text{ s}^{-1}} -\text{PO}_3\text{H}^- + \text{H}_3\text{O}^+, K_1 = 2 \times 10^{-4} \text{ mol/L}$ $-\text{PO}_3\text{H}^- + \text{H}_2\text{O} \xrightleftharpoons[k_{-2}=10^8 \pm 10^{10} \text{ L/(mols)}]{k_2=5 \times 10^{-3} \pm 5 \times 10^{-1} \text{ s}^{-1}} -\text{PO}_3\text{H}^- + \text{OH}^-, K_2 = 5 \times 10^{-11} \text{ mol/L}$
–PO <sub>3</sub> H <sup>–</sup>	$-\text{PO}_3\text{H}^- + \text{H}_2\text{O} \xrightleftharpoons[k_{-1}=10^{10} \pm 10^{11} \text{ L/(mols)}]{k_1=10^3 \pm 10^4 \text{ s}^{-1}} -\text{PO}_3^{2-} + \text{H}_3\text{O}^+, K_1 = 10^{-7} \text{ mol/L}$ $-\text{PO}_3^{2-} + \text{H}_2\text{O} \xrightleftharpoons[k_{-2}=10^8 \pm 10^{10} \text{ L/(mols)}]{k_2=10^1 \pm 10^3 \text{ s}^{-1}} -\text{PO}_3\text{H}^- + \text{OH}^-, K_2 = 10^{-7} \text{ mol/L}$
–SO <sub>3</sub> H	$-\text{SO}_3\text{H} + \text{H}_2\text{O} \xrightleftharpoons[k_{-1}=3 \times 10^{10} \text{ L/(mols)}]{k_1=10^9 \text{ s}^{-1}} -\text{SO}_3^- + \text{H}_3\text{O}^+, K_1 = 3 \times 10^{-2} \text{ mol/L}$ $-\text{SO}_3^- + \text{H}_2\text{O} \xrightleftharpoons[k_{-2}=10^{10} \text{ L/(mols)}]{k_2=3 \times 10^{-3} \text{ s}^{-1}} -\text{SO}_3\text{H} + \text{OH}^-, K_2 = 3 \times 10^{-13} \text{ mol/L}$
≡ N	$\equiv \text{N} + \text{H}_2\text{O} \xrightleftharpoons[k_{-1}=3 \times 10^{10} \text{ L/(mols)}]{k_1=3 \times 10^6 \text{ s}^{-1}} \equiv \text{NH}^+ + \text{OH}^-, K_1 = 10^{-4} \text{ mol/L}$ $\equiv \text{NH}^+ + \text{H}_2\text{O} \xrightleftharpoons[k_{-2}=10^{10} \text{ L/(mols)}]{k_2=10^0 \text{ s}^{-1}} \equiv \text{N} + \text{H}_3\text{O}^+, K_2 = 10^{-10} \text{ mol/L}$
= NH, –NH <sub>2</sub>	$= \text{NH} + \text{H}_2\text{O} \xrightleftharpoons[k_{-1}=3 \times 10^{10} \text{ L/(mols)}]{k_1=3 \times 10^7 \text{ s}^{-1}} = \text{NH}_2^+ + \text{OH}^-, K_1 = 10^{-3} \text{ mol/L}$ $= \text{NH}_2^+ + \text{H}_2\text{O} \xrightleftharpoons[k_{-2}=10^{10} \text{ L/(mols)}]{k_2=10^{-1} \text{ s}^{-1}} = \text{NH} + \text{H}_3\text{O}^+, K_2 = 10^{-11} \text{ mol/L}$

### Appendix B. Method of solving the equations for the CVC model.

For each of the four layers composing the studied system let us reduce the initial boundary value problem (Eq. (12)) to a two-point boundary value problem. We rewrite Eq. (13) as follows:

$$\frac{dc_i}{dX} = f(c_i) \quad (\text{B1})$$

where  $X = \frac{x}{d}$  is a dimensionless spatial coordinate and  $d$  is the length of the layer.

Since the problem is a stationary problem, we still have the usual differential equation, which describes the fluxes as independent of the space coordinate:

$$\frac{dj_i(X)}{dX} = v_i \quad (\text{B2})$$

We represent the vector composed of the unknown initial functions by  $Y = (c_i(X), j_i(X))$ . With the vector  $Y(X)$ , the system of differential equations in Eqs. (B1) and (B2) can be rewritten in the usual standard form:

$$\frac{dY(X)}{dX} = f(Y(X)) \quad (\text{B3})$$

The local chemical equilibrium condition allows us to exclude hydrogen ion from layers to the left of bipolar boundary and hydroxyl ions from the layers to the right of the bipolar boundary, hence the dimension of Eq. (B3) is  $n = 12$ . For the boundary points  $X_b = 0, X_l = 1, X_0 = 2, X_r = 3, X_a = 4$  we can write:

$$\begin{aligned}
 & \varphi^{(k)} = c_i - c_i^b; k = 1, 2, 3 \\
 X_b & \varphi^{(4)} = \sum_i c_i \\
 & \varphi^{(5)} = \sum_i c_i - c_f^a \\
 X_l & \varphi^{(6)} = c_i(1-0)e^{\psi^{(1-0)}} - c_i(1+0)e^{\psi^{(1+0)}} \\
 & \varphi^{(k)} = \bar{j}_i - j_i; k = 7, 8, 9 \\
 & \varphi^{(10)} = \sum_i c_i - c_f^a \\
 & \varphi^{(11)} = c_i(2-0)e^{\psi^{(2-0)}} - c_i(2+0)e^{\psi^{(2+0)}} \\
 X_0 & \varphi^{(12)} = \bar{j}_W - \frac{k_\Sigma \varepsilon \varepsilon_0}{\beta} (e^{\beta E_m(\eta_b)} - e^{\beta E_m(0)}) \\
 & \varphi^{(k)} = \bar{j}_i - \bar{j}_i; k = 13, 14, 15 \\
 & \varphi^{(16)} = \sum_i c_i - c_f^c \\
 X_r & \varphi^{(17)} = c_i(3-0)e^{\psi^{(3-0)}} - c_i(3+0)e^{\psi^{(3+0)}} \\
 & \varphi^{(k)} = \bar{j}_i - j_i; k = 18, 19, 20 \\
 & \varphi^{(k)} = c_i - c_i^a; k = 21, 22, 23 \\
 X_a & \varphi^{(24)} = \sum_i c_i
 \end{aligned} \tag{B4}$$

We introduce vector  $F \equiv (\varphi^{(1)}, \varphi^{(2)}, \dots, \varphi^{(24)})^T$  and vector  $\theta \equiv (\theta_1, \theta_2, \dots, \theta_{24})^T = (c_i(X_j), j_i(X_j))^T, i = A, C, W; j = l, 0, r$ .

It is necessary to find the vector  $\theta$  such that it represents the initial values for the unknown functions  $c_i(X), j_i(X)$  in

order to make the errors in  $F \equiv (\varphi^{(1)}, \varphi^{(2)}, \dots, \varphi^{(k)})^T$  vanish at the left and right boundaries. A simple unmodified shooting method was applied.

$$F(0) = 0$$

The problem was solved by the classical Newton method:

$$\begin{aligned}
 Aw_p &= B, \\
 A &= F'(\theta_p), \\
 B &= -F(\theta_p), \\
 \theta_{p+1} &= \theta_p + w_p,
 \end{aligned}$$

where  $F'(\theta_p)$  is the matrix of derivatives of the function  $F$  at the  $p$ th iterative step.

Numerical calculation of the matrix of derivatives  $F'$

$$F' = \begin{bmatrix} \frac{\partial \varphi^{(1)}}{\partial \theta_k} \\ \vdots \\ \frac{\partial \varphi^{(24)}}{\partial \theta_k} \end{bmatrix}$$

is carried out by approximating the derivatives with discrete differences with second-order accuracy:

$$\frac{\partial \varphi^{(i)}}{\partial \theta_k} \approx \frac{\varphi^{(i)}(\dots, \theta_k + \Delta, \dots) - \varphi^{(i)}(\dots, \theta_k - \Delta, \dots)}{2 \Delta}$$

on a four-point grid, which requires four additional procedures for integrating Eq. (B3) at each  $p$ th iterative step.

Iteration is performed until the following condition is no longer fulfilled:

$$\|\theta_{p+1} - \theta_p\| + \|F(\theta_{p+1})\| < \varepsilon$$

where  $\varepsilon = 10^{-4} - 10^{-5}$  is the designated accuracy for the solution to the system of nonlinear algebraic equations.